Sources and transformation mechanisms of atmospheric particulate bound mercury revealed by mercury stable isotopes

Chen Liu[†,‡], Xuewu Fu[*,†], Yue Xu[†], Hui Zhang[†,‡], Xian Wu[†,‡], Jonas Sommar[†], Leiming Zhang[§], Xun Wang[†], Xinbin Feng[†,‡]

[†]State Key Laboratory of Environmental Geochemistry, Institute of Geochemistry, Chinese Academy of Sciences, Guiyang, 550081, China

[‡]University of Chinese Academy of Sciences, Beijing, 100049, China

[§]Air Quality Research Division, Science and Technology Branch, Environment and Climate Change Canada, Toronto, Ontario, Canada

*Corresponding Authors: fuxuewu@mail.gyig.ac.cn

Abstract: This study examined the isotope composition of Particulate bound mercury (PBM) in ten Chinese megacities and explored the associated sources and transformation mechanisms. PBM in these cities were characterized by negative δ^{202}Hg (means: -2.00 to -0.78‰), slightly negative to highly positive Δ^{199}Hg (means: -0.04 to 0.47‰), and slightly positive Δ^{200}Hg (means: 0.02 to 0.06‰) values. The positive PBM Δ^{199}Hg signatures were likely caused by physiochemical reactions in aerosols. The Δ^{199}Hg/Δ^{201}Hg ratio varied from 0.94 to 1.39 in the cities and increased with the corresponding mean $\Delta^{199}Hg_{PBM}$ value. We speculate that, in addition to photoreduction of oxidized Hg, other transformation mechanisms in aerosols (e.g., isotope exchange, complexation, and oxidation that express nuclear volume effects) also shape the $\Delta^{199}Hg_{PBM}$ signatures in the present study. These processes are likely enhanced in the presence of strong gas-particle partitioning of gaseous oxidized Hg (GOM), and elevated levels of redox active metals (e.g., Fe), halides and elemental carbon. Based on $\Delta^{200}Hg_{PBM}$ data presented in this and previous studies, we estimate that large proportions (~47%) of PBM were sourced from oxidation of gaseous elemental Hg followed by partitioning of GOM onto aerosols globally, indicating transformation of Hg(0) to PBM as an important sink of atmospheric Hg(0).

Keywords: PBM, urban atmosphere, stable Hg isotope, MIF, MIE, NVE, heterogeneous Hg reactions, sources

SYNOPSIS: This work provides new knowledge on the MIF of Hg isotopes in aerosols and the sources of particulate bound mercury

TOC abstract:

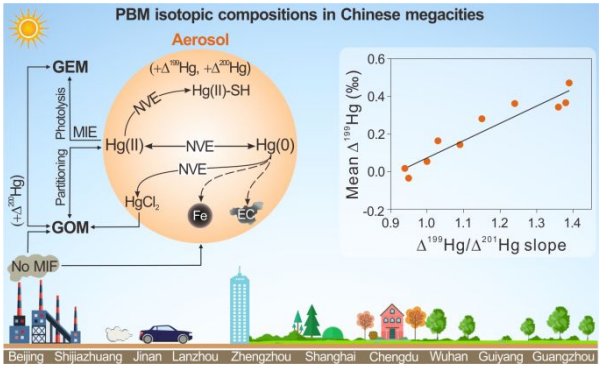

1. Introduction

Mercury (Hg) in the atmosphere mainly exists in the forms of gaseous elemental mercury (GEM or Hg(0)), gaseous oxidized mercury (GOM), and particulate bound mercury (PBM). Hg directly emitted into the atmosphere from anthropogenic and natural sources or reemitted from previously deposited Hg is mostly in the form of Hg(0).[1] Hg(0) is much less susceptible to dry and wet removal processes as compared with GOM and PBM and is readily transported over a hemispherical scale. Oxidation of Hg(0) to Hg (II) (GOM and PBM) in the atmosphere followed by Hg (II) wet and dry deposition is perceived as one of the major sinks of atmospheric Hg(0).[2, 3] Hence, a complete understanding of the sources and transformation mechanisms of speciated atmospheric Hg is critical for assessing Hg cycling in the atmosphere.

Recent studies have improved our understanding of the atmospheric gas-phase Hg redox schemes,[4-7] while the knowledge of reactions in aqueous and heterogeneous phases remains largely limited.[7, 8] In current global atmospheric Hg models, Hg(0) oxidation is assumed to be mainly induced by Br and OH, and then the gaseous oxidized Hg could be either reduced back to Hg(0), persist as GOM in the atmosphere in relatively photochemically and thermally stable Hg(I, II) forms, or captured by aerosols and cloud droplets.[2, 3, 8, 9] Once incorporated into aerosols and cloud droplets, Hg(I, II) can undergo many physiochemical transformation processes.[7] Among viable processes, aqueous-phase Hg(II) photoreduction is frequently considered in modeling studies and supposed to play important roles in the atmospheric chemistry of Hg.[2, 3, 8] On the other hand, other in-aerosol processes such as re-oxidation, complexation and adsorption, which allow Hg(II) to be retained as PBM, are frequently neglected in global modelling because of deficient knowledge.[3, 7, 8]

Hg stable isotopes can help constrain its sources and transformation mechanisms in the natural environment because physicochemical processes induce mass dependent fractionation (MDF, δ^{202}Hg signature) and odd- and even-mass independent fractionation (MIF, Δ^{199}Hg, Δ^{200}Hg and Δ^{201}Hg signatures). MDF of Hg isotopes can be caused by many physicochemical processes, including reduction, methylation/demethylation, sorption, and evaporation.[10] Large odd-MIF of Hg isotopes are mainly associated with photochemical redox reactions due to the magnetic isotope effect (MIE).[11-15] Small magnitudes of odd-MIF (e.g., <0.6‰) have also been observed in abiotic dark Hg(II) reduction, Hg(II) complexation with thiol, and abiotic dark Hg(0) oxidation (mainly due to equilibrium isotope exchange) experiments, which are accompanied by a discernable Δ^{199}Hg/Δ^{201}Hg regression slope of ~1.6 compared to the MIE (slope of ~1.0) due to the nuclear volume effect (NVE).[16-18] Even-MIF anomalies are mainly observed in atmospheric samples and are assumed to be exclusively produced during atmospheric redox reactions at high altitudes.[19-22] Recently, measurements of the Hg isotopic composition in atmospheric aerosols have been carried out at urban,[23-26] remote,[27, 28] oceanic,[28-30] and polar sites[31, 32] worldwide, from which it was

proposed that industrial emissions, subsequent in-aerosol photoreduction, and conversion of Hg(0) to PBM are crucial factors regulating the variations in PBM isotopic composition.[27, 28, 32, 33] Oxidation processes were also speculated to be of potential importance in an oceanic study, but the detailed mechanisms remained to be largely unknown.[29] Hence, the links between heterogeneous Hg reactions in aerosols and PBM isotopic signature have yet to be established.

Considering the crucial roles PBM plays in atmospheric Hg cycling,[7, 8, 34] further investigation of Hg transformation at the interface of and within aerosols using diversified approaches are warranted.[7, 8] In the present study, we measured the isotopic composition of PBM in ten Chinese megacities. PBM concentrations in Chinese urban areas are generally highly elevated and represent the major Hg species scavenged from the atmosphere in China.[35, 36] The PBM isotope signatures together with the chemical characteristics of $PM_{2.5}$ and meteorological parameters were used to explore the effect of in-aerosol Hg transformation on the MIF of PBM. Finally, PBM sourced from atmospheric oxidation of Hg(0) followed by aerosol scavenging processes is constrained using a Δ^{200}Hg mixing model.

2. Materials and methods

2.1 PBM sampling

PBM samples were collected at downtown sites in ten megacities in China (i.e., Beijing, Shijiazhuang, Jinan, Lanzhou, Zhengzhou, Shanghai, Chengdu, Wuhan, Guiyang, and Guangzhou) (Figure S1). Detailed information of the sampling sites and the cities can be found in Fu et al..[37] $PM_{2.5}$ samples were collected on quartz fiber filters (8×10 in sheet, Munktell, Sweden) using high-volume $PM_{2.5}$ samplers (ASM-1, Guangzhou Minya, China) at a flow rate of 1.0 m^3 min^{-1}. Before sampling, quartz filters were preheated at 500 °C for 6 h to minimize the Hg blank in filters. In this study, $PM_{2.5}$ samples were collected on a daily basis in both summer and winter campaigns. For the wintertime campaigns, $PM_{2.5}$ samples were collected simultaneously from 5 to 14 January 2018 in Beijing, Shijiazhuang, Jinan, Lanzhou, and Zhengzhou, and from 19 to 26 January 2018 in Shanghai, Chengdu, Wuhan, Guiyang, and Guangzhou. For the summertime campaigns, $PM_{2.5}$ samples were collected simultaneously from 29 June to 6 July 2018 in Shijiazhuang, Jinan, Zhengzhou, Guiyang, and Guangzhou, and were collected simultaneously from 27 July to 6 August 2018 in the remaining five cities (Table S1). Filters were sealed carefully in polyethylene bags immediately after the completion of field sampling and kept frozen (-18 °C) before further sample processing.

2.2 Sample processing and analysis

A small piece (~10%) of filters was cut off from the large filter sheets (8×10 inch) using a Teflon scissor for the analysis of PBM concentration and isotope composition. The filters were combusted in a Hg-free oxygen flow in a quartz tube (25 mL min^{-1}), and then PBM in $PM_{2.5}$ was

thermally released as Hg(0) which was subsequently preconcentrated into 5 mL of 40% HNO_3/HCl mixed trapping solution (v/v, 2:1).[38] Hg concentration in trapping solution was measured using a cold vapor atomic fluorescence spectroscopy (CVAFS) method. PBM concentration in ambient air was calculated by dividing the Hg mass in trapping solution by the sampling air volume through the filter piece.

Isotope ratios of Hg in trapping solution were determined using cold vapor multicollector inductively coupled plasma mass spectrometry (MC-ICPMS, Nu-Plasma, UK).[28] MDF and MIF values of PBM are reported in delta notation (δ) and capital delta (Δ) in per mil (‰), respectively, which are calculated using the following equations:[39]

$$\delta^{xxx}Hg = \left[\frac{\left(^{xxx}Hg/^{198}Hg\right)_{sample}}{\left(^{xxx}Hg/^{198}Hg\right)_{NIST-3133}} - 1\right] \times 1000 \quad (1)$$

$$\Delta^{xxx}Hg = \delta^{xxx}Hg - \beta \times \delta^{202}Hg \quad (2)$$

where *xxx* is the mass number of Hg isotopes (199, 200, 201, 202, and 204), *sample* is the PBM collected in the present study, *NIST-3133* is the bracketing NIST SRM 3133 Hg standard reference during analysis, and β is 0.2520, 0.5024, 0.7520, and 1.493 for ^{199}Hg, ^{200}Hg, ^{201}Hg, and ^{204}Hg, respectively, which are determined from the kinetic MDF law.[39]

The recoveries of sample processing were investigated by combustions of CRM BCR-482 (lichen), NSIT SRM 2711a (Montana soil), and NIST SRM 1648 (urban particulate matter), which showed mean recoveries of 87.9 ± 6.6% (1sd, n = 6), 96.0 ± 4.2% (1sd, n = 6), and 91.9 ± 10.8% (1sd, n = 19), respectively. Combustion of preheated filters showed a mean system blank of 0.09 ± 0.05 ng mL^{-1} (1sd, n = 15) for the field sampling and processing, which accounted for < 10% of the collected PBM in trap solutions. Isotope ratios of Hg in NIST SRM 3177 ($HgCl_2$ solution), NIST SRM 2711a, and CRM BCR 482 were routinely measured during the analysis of PBM isotopic composition. The measured Hg isotopic composition of the reference materials agree well with those reported in previous studies (Table S2).[12, 40] The reported analytical uncertainty of the PBM isotopic composition in this study is the higher 2sd value of either NIST SRM 3177 or repeated analysis of PBM samples.

2.3 Ancillary parameters

Each filter was conditioned and weighted before and after field sampling using a constant temperature and humidity weighting system (YCT-H, YoCredit Electronics & Technology Co, Ltd, Qingdao, China), and the mass difference is used to calculate the $PM_{2.5}$ mass concentration of each sample by dividing the air sampling volume. Organic carbon (OC) and elemental carbon (EC) in $PM_{2.5}$ samples were detected using an OC-EC aerosol analyzer (Sunset Laboratory, Inc., USA). Water-soluble anions (including Cl^{-1}) in $PM_{2.5}$ were measured by Milli-Q water extraction of filters followed by a detection of iron chromatography (ICS-900, Dionex, USA), and trace elements

(including Fe and Cd) were measured using acid digestion followed by a detection of inductively coupled plasma–mass spectrometry (ICP-MS, PerkinElmer, USA), following the method described in a previous study.[41] An analysis of trace elements in NIST SRM 1648 showed mean recoveries of 91.7 ± 9.5% and 93.2 ± 10.8% (1sd, n = 19) for Fe and Cd, respectively. Meteorological parameters were obtained from the local weather stations in the investigated cities.

3. Results and discussion

3.1 PBM concentration and isotope composition

City-specific mean PBM concentrations ranged from 33.6 to 158 pg m^{-3} (n = 10, Table S3), and the overall mean value from the 10 cities was 74.9 ± 82.9 pg m^{-3} (1sd, n = 130) during the study period. This mean value was approximately 1.5 times of that obtained from Chinese rural areas and more than one order of magnitude higher than those in North America and Europe.[35, 42] The mean concentration of PBM in the cities was not correlated with that of $PM_{2.5}$ or EC (ANOVA, $p > 0.05$ for both), but significantly positively correlated with that of OC ($r^2 = 0.89$, $p < 0.01$) (Figure S2). The strong correlation between PBM and OC is similar to the observations in precipitation samples.[43] High mass fraction of OC in aerosol is conducive to GOM adsorption by aerosol or aerosol water and complexation of Hg(II) inside aerosol,[44, 45] which may therefore represent a major factor controlling the PBM variation among the investigated cities.

Isotopic compositions of daily PBM samples collected in the 10 cities exhibited large variations with δ^{202}Hg, Δ^{199}Hg, and Δ^{200}Hg values being in the range of -3.28 to 0.41‰, -0.67 to 0.94‰, and -0.13 to 0.16‰ (n = 125), respectively (Table S1). A minor fraction of PBM samples (16% of the total collected samples) were characterized by negative Δ^{199}Hg values, which were mainly observed in winter campaign (Table S1). City-specific mean δ^{202}Hg, Δ^{199}Hg, and Δ^{200}Hg values of PBM during the study period ranged from -2.00 to -0.78‰ , -0.04 to 0.47‰ , and 0.02 to 0.06‰ (n = 10) , respectively, while the overall mean from the whole 10 cities were -1.16‰, 0.22‰, and 0.05‰, respectively (Figure 1 and Table S3). PBM isotope compositions observed in the present study align well with the pool of global PBM data, which are characterized by significantly negative δ^{202}Hg (means = -1.64 to -0.69‰), slightly negative to significantly positive Δ^{199}Hg (means = -0.21 to 0.83‰), and positive Δ^{200}Hg signatures (0.01 to 0.14‰) (Table S3),[23-30, 46, 47] with the exception of the observations in Polar regions (mean δ^{202}Hg = 0.03 to 1.05‰, mean Δ^{199}Hg = -0.38 to -0.28‰, mean Δ^{200}Hg = -0.01 to 0.00‰, n = 2) (Table S3).[31, 32] By comparison, PBM at urban sites worldwide showed relatively lower Δ^{199}Hg and Δ^{200}Hg values as compared to observations at Chinese rural sites, in marine air, and at a coastal site in the United States (Figure 1). The isotope composition in flue gases and other primary anthropogenic emissions shows slightly negative to near zero values of Δ^{199}Hg and Δ^{200}Hg.[48-50] The lower values of PBM Δ^{199}Hg and Δ^{200}Hg at urban

sites would therefore suggest relatively higher contributions from primary anthropogenic emissions (PBM emissions and adsorption of GOM emitted from anthropogenic sources) to PBM in the urban areas.[34, 51]

The isotope composition of PBM in this and previous studies are generally distinguishable from those of Hg(0) and GOM (Figure 1 and Table S3). For example, the isotope composition of Hg(0) at urban and rural sites in China showed relatively higher δ^{202}Hg ($mean_{urban}$ = -0.57 ± 0.38‰, $mean_{rural}$ = 0.09 ± 0.39‰) and lower Δ^{199}Hg ($mean_{urban}$ = -0.06 ± 0.06‰, $mean_{rural}$ = -0.12 ± 0.04‰) and Δ^{200}Hg ($mean_{urban}$ = -0.01 ± 0.04‰, $mean_{rural}$ = -0.04 ± 0.02‰) values.[37, 46, 52, 53] Mean Δ^{199}Hg and Δ^{200}Hg values of GOM at Grand Bay, United States and Pic Du Midi, France ranged from -0.11 to 0.44‰ and 0.15 to 0.18‰, respectively.[22, 27] The mechanisms underlying the discernible isotope signatures (especially the MIF) among atmospheric Hg species, although not well constrained, were proposed to be mainly associated with photochemical reactions in the atmosphere.[19, 20, 22, 28, 33]

3.2 Seasonal variations in PBM concentration and isotope composition

City-specific mean PBM concentrations in winter (62.7 to 245 pg m^{-3}) were 1.5 to 4.5 times of those in summer in nine cities and were 20% lower in one city (Shanghai) during the study period (Figure 2). Such a seasonal variation in PBM concentration (i.e., higher level in winter than summer) is consistent with those previously reported for urban and rural locations in mainland China.[35] The mean PBM/$PM_{2.5}$ ratio and PBM/EC ratio were also higher in winter (PBM/$PM_{2.5}$ = 1.03 ± 0.48 pg m^{-3}/μg m^{-3}, PBM/EC = 94.1 ± 42.6 pg m^{-3}/μg m^{-3}) than in summer (PBM/$PM_{2.5}$ = 0.67 ± 0.38 pg m^{-3}/μg m^{-3}, PBM/EC = 62.0 ± 29.8 pg m^{-3}/μg m^{-3}) at most sites (Figure 2). These observations indicate an enrichment of Hg in atmospheric particles in winter, likely due to increasing gas-particle partitioning of GOM, decreasing photochemical losses of Hg from particles under cold and darker conditions, and/or changing anthropogenic emission sources (Figure 2).[3, 34, 51]

During the study period, city-specific mean PBM δ^{202}Hg values ranged from -1.83 to -0.74‰ (mean = -1.24‰, n = 10) in summer, which were lower than the corresponding values in winter in most cities expect in Shanghai and Guiyang (from -2.42 to -0.60‰, mean= -1.08‰, n = 10) (Figure 2). Mean PBM Δ^{199}Hg values in summer (0.07 to 0.42‰) were higher than the corresponding observations in winter (-0.19 to 0.28‰) at seven urban sites (Figure 2). A previous study investigating diel PBM isotope compositions in Beijing, China suggested that stronger solar radiation would increase Δ^{199}Hg because of increasing photoreduction processes.[33] Such a hypothesis could partially explain the relatively higher PBM Δ^{199}Hg in summer in the seven cities mentioned above. However, the opposite seasonal pattern was observed in three cities (Jinan, Lanzhou, and Zhengzhou) with higher PBM Δ^{199}Hg and much weaker solar radiation intensity in winter than in summer (Figure 2), indicating that other atmospheric reactions likely also played important roles in shaping MIF of PBM in urban areas (more discussion in Section 3.3 below).

The relationships between Δ^{199}Hg and PBM/$PM_{2.5}$, PBM/EC, and PBM/Cd ratios were analyzed for revealing potential transformation mechanism of PBM. EC and Cd in the atmosphere are mainly derived from anthropogenic sources, and Cd shares approximately 80% of the anthropogenic sources for Hg.[54, 55] Therefore, decreasing PBM/$PM_{2.5}$, PBM/EC, and PBM/Cd ratios would indicate potential losses of Hg from aerosols due to photoreduction and volatilization processes. PBM Δ^{199}Hg significantly negatively correlated with PBM/EC and PBM/Cd ratios (ANOVA, r^2 = 0.45 to 0.59, $p < 0.05$) in summer, but only weakly and insignificantly negatively correlated with PBM/$PM_{2.5}$ ($r^2 = 0.19$, $p = 0.21$) (Figure S3). The PBM samples collected in summer (n = 56) displayed a Δ^{199}Hg/Δ^{201}Hg slope of 1.04 (Figure S4), which was within the range of those (1.00 to 1.12) derived from photoreduction of Hg(II) complexed with DOC and soot particles and anthropogenic sources.[11, 56, 57] These findings suggest photoreduction of PBM was likely responsible for the positive Δ^{199}Hg values in summer in these cities. In contrast, no significant correlations were observed between PBM Δ^{199}Hg and PBM/$PM_{2.5}$, PBM/EC and PBM/Cd ratios in winter, and the Δ^{199}Hg/Δ^{201}Hg slope was 1.20 (Figure S3 and S4). We reason that the partitioning of GOM to PBM increases during winter and this addition of Hg(II) is then processed to a greater extent by reactions within aerosols (more discussions in Section 3.3 below).[7, 34]

3.3 Odd-Hg MIF induced by mercury transformations in aerosols

PBM in the atmosphere is mainly derived from primary anthropogenic emissions and gas-particle partitioning of GOM,[8, 34, 51] whereas the adsorption and oxidation of Hg(0) on aerosol surfaces are generally considered less relevant due to its low solubility in liquid aerosols,[58] low uptake by soot,[59] and weak reactivity at the interface.[60] The MIF of Hg isotopes and Δ^{199}Hg/Δ^{201}Hg ratios can be potential tracers of Hg transformations. In the present study, we observed that city-specific mean Δ^{199}Hg/Δ^{201}Hg ratios of PBM varied noticeably from 0.94 ± 0.12 to 1.39 ± 0.11 (Figure 3), and the mean Δ^{199}Hg of PBM increased linearly with this ratio (ANOVA, $r^2 = 0.90$, $p <$ 0.01, Figure S5).

The much higher than unity Δ^{199}Hg/Δ^{201}Hg ratios of PBM observed in some cities (e.g., 1.24 to 1.39 in Shijiazhuang, Jinan, Lanzhou, and Zhengzhou) were not likely inherited from GOM during gas-particle partitioning because available global data showed Δ^{199}Hg/Δ^{201}Hg ratios of GOM being around 1.0.[22, 27] Global source materials and anthropogenic PBM emissions generally have small magnitude of odd-MIF and a Δ^{199}Hg/Δ^{201}Hg ratio of ~1.0,[61] and therefore should not be the cause of the observed high Δ^{199}Hg/Δ^{201}Hg ratios. Generally, large MIF of odd-Hg isotopes are mainly induced by the magnetic isotope effect (MIE) during photochemical redox reactions of Hg in the environment. Photoreduction of Hg(II) may result in either (+)MIE (positive Δ^{199}Hg in reactant) or (-)MIE (negative Δ^{199}Hg in reactant), depending on the complexes of Hg(II) and reaction conditions.[15, 56, 62] Experimental studies on the photoreduction of Hg(II) in fresh waters

(DOC complexed), water-saturated soot particles, and soils show (+)MIE with $\Delta^{199}Hg/\Delta^{201}Hg$ ratios ranging from 1.0 to 1.12,[11, 56, 57, 62, 63] and this explains well the $\Delta^{199}Hg/\Delta^{201}Hg$ ratios (0.94 to 1.15) observed in six out of the ten cities (Figure 3). Photoreduction of Hg(II) complexed with S containing ligands can potentially generate high $\Delta^{199}Hg/\Delta^{201}Hg$ ratios of up to 1.34 to 1.46 accompanied by significantly negative $\Delta^{199}Hg$ in reactant Hg(II) due to (-)MIE.[56, 62] Photochemical gas-phase oxidation of Hg(0) by atomic Br and Cl has $\Delta^{199}Hg/\Delta^{201}Hg$ ratios of 1.64 and 1.89, respectively, but would likely result in negative $\Delta^{199}Hg$ in PBM following the adsorption of GOM reaction product by particles.[12] These experimental results are in contrast, at least to a certain extent, with the observations in Shijiazhuang, Jinan, Lanzhou, and Zhengzhou (e.g., high $\Delta^{199}Hg/\Delta^{201}Hg$ ratios of 1.24 to 1.39 and highly positive mean $\Delta^{199}Hg$ of 0.34 to 0.47‰, Figure 3). A previous study showed that $\Delta^{199}Hg/\Delta^{201}Hg$ ratio increased from 1.19 to 1.31 with Hg/DOC ratio increasing from 34.6 to 8330 ng/mg during aqueous Hg(II) photoreduction.[13] Given the fractions (mean: 67%) of water soluble OC in total OC in aerosols,[64] we estimated that the mean water soluble Hg/DOC ratio in aerosols would not exceed 24 ng/mg in these cities (Table S1), which corresponds to the lowest Hg/DOC experiments in the previous study.[13] Thus, Hg/DOC ratio was likely not the control factor for the observed high $\Delta^{199}Hg/\Delta^{201}Hg$ ratios in some cities. MIF of Hg isotopes during dark abiotic Hg(II) reduction dominated by NVE is characterized by a $\Delta^{199}Hg/\Delta^{201}Hg$ ratio of ~1.6.[13, 17] This process, however, is expected to play a minor role because of its fairly slow reaction rates in solutions and aerosols and negative $\Delta^{199}Hg$ signatures in Hg(II) reactant.[13, 65]

In the present study, we found the $\Delta^{199}Hg/\Delta^{201}Hg$ ratio in the 10 cities negatively correlated with air temperature (ANOVA, $r^2 = 0.66$, $p < 0.01$), and positively correlated with water-soluble Cl^-, total Fe, and EC concentrations in aerosols (ANOVA, $r^2 = 0.54$ to 0.64, $p < 0.01$ or 0.05) (Figure S6). Low air temperatures enhance the gas-particle partitioning of GOM,[34] high levels of Cl^- promote Hg(0) oxidation,[66] and high Fe (partial in Fe_2O_3 form) and EC (S-rich) contents facilitate the uptake of Hg(0) in aerosols.[67, 68] These factors together can facilitate the physiochemical reactions of Hg compounds in aerosols following the strong gas-particle partitioning of GOM. Recent modelling studies suggested that the major Hg(II) products derived from atmospheric Hg(0) gas-phase oxidation are mainly complexed with -BrONO, -BrOOH, -BrOH, and -OH,[4, 8] whereas Hg compounds in airborne particles are expected to include Hg(0), Hg(I), $HgCl_2$, HgS, and HgO.[69, 70] We therefore hypothesize that substantial physiochemical transformations of Hg compounds may exist in aerosols following the gas-particle partitioning of GOM. This hypothesis is used here to interpret the odd-MIF of PBM (Figure 4).

Following the partitioning of GOM into aerosols, Hg(II) can undergo photoreduction to form Hg(0), which is either released back to the atmosphere or retained in aerosols. The photoreduction of Hg(II) is expected to drive a large positive $\Delta^{199}Hg$ shift and generate a $\Delta^{199}Hg/\Delta^{201}Hg$ ratio of

~1.0 in reactant Hg(II) in aerosols due to (+)MIE. [11, 56, 62] In addition to Hg(II) photoreduction, a fraction of Hg(II) is likely complexed with thiol functional groups, and this equilibrium process results in a small positive Δ^{199}Hg shift (e.g., < 0.1‰) in thiol bound Hg(II) relative to reactant Hg(II) and a Δ^{199}Hg/Δ^{201}Hg ratio of ~1.6 due to NVE.[16] The thiol bound Hg(II) displays a limited reactivity towards photoreduction and therefore tends to be retained in aerosols.[71] More importantly, we propose that the redox reactions involving Hg compounds in aerosols are also crucial for the odd-MIF of PBM (Figure 4). Once reduced, Hg(0) in aerosols may be rapidly re-oxidized back to Hg(II), especially in the presence of abundant Cl^- (through production of reactive chlorine species or complex Hg(II) product), trace metals in higher oxidation states (e.g., Fe_2O_3), and organic and humic acid, as observed in previous studies.[18, 66, 68] The coexistence of Hg(0) and Hg(II) in aerosols facilitates the Hg(0)-Hg(II) isotope exchange which in turn generates a Δ^{199}Hg/Δ^{201}Hg ratio of ~1.6 due to NVE and a positive Δ^{199}Hg shift (up to 0.18‰) in Hg(0) retained in aerosols.[18] In addition, reactive chloride readily oxidizes Hg(0) in liquid aerosols (triggered by OH and/or ozone),[68] which has been observed to produce large MIF of odd-Hg isotopes ($E^{199}Hg_{reactant-product}$ = 0.13 to 0.44‰) and Δ^{199}Hg/Δ^{201}Hg ratios of 1.6 to 1.9 by gas-phase and aqueous experiments.[12, 72] As highlighted by a recent modelling study,[8] a substantial fraction of photostable $HgCl_2$ (negative Δ^{199}Hg) produced in this manner would be partitioned into the gas phase, which in turn leads to an increase of Δ^{199}Hg and Δ^{199}Hg/Δ^{201}Hg ratio in the aerosol Hg pool. The remaining fractions of Hg(0) could be retained in aerosols by adsorption to elemental carbon (EC) soot and Fe_2O_3 nanoparticles,[69, 73, 74] preserving the positive MIF signatures of Hg(0) in aerosols (Figure 4). The above hypothesis is supported by the observed effects of water-soluble Cl^-, total Fe, and EC in aerosols on the variations in Δ^{199}Hg/Δ^{201}Hg ratio (Figure S6). These factors together facilitate the physiochemical reactions of Hg compounds in aerosols (e.g., Hg(II) thiol complexation, reactive chloride oxidation, and nanoparticle uptake of Hg(0)), that potentially lead to positive shifts of odd-Hg MIF and increased Δ^{199}Hg/Δ^{201}Hg ratio in PBM. Based on a binary mixing model of NVE and MIE fractionation and their respective typical Δ^{199}Hg/Δ^{201}Hg ratios of 1.6 and 1.0 (Text S1 and Figure S7), we roughly estimate that the shift of PBM Δ^{199}Hg due to the NVE in Shijiazhuang, Jinan, Lanzhou, and Zhengzhou were on average 0.26‰ (0.00 to 0.55‰), 0.31‰ (0.00 to 0.70‰), 0.46‰ (0.00 to 0.67‰), and 0.16‰ (0.00 to 0.41‰), respectively. These values are somewhat higher than those produced during Hg(II) thiol complexation and Hg(0)-Hg(II) isotope exchange experiments (Δ^{199}Hg <0.2‰),[16, 18] but within the range of those produced during Cl-triggered Hg(0) oxidation (Δ^{199}Hg up to ~1.2‰).[12, 72] We caution that several Hg(II) photoreduction experiments have reported Δ^{199}Hg/Δ^{201}Hg ratios of higher than 1.0 for (+)MIE,[13, 62] and therefore the potential contributions of the Hg(II) photoreduction to the elevated Δ^{199}Hg/Δ^{201}Hg ratios in the present study should be not

ruled out. For example, using a $\Delta^{199}Hg/\Delta^{201}Hg$ ratio of 1.19 for (+)MIE that resemble the Hg/DOC ratio in aqueous aerosols in this study would predict smaller contributions of NVE to the odd-Hg MIF in these cities (Text S1).[13] Nevertheless, high $\Delta^{199}Hg/\Delta^{201}Hg$ ratios (e.g., 1.24 to 1.39) observed in some cities in the present study suggest that photochemical Hg(II) reduction is not likely the exclusive origin of the odd-Hg MIF in aerosols, and other in-aerosol heterogeneous Hg reactions should be also considered to interpret the odd-MIF signatures of PBM in the urban environment. Further studies on the mechanisms of odd-MIF and diagnostic $\Delta^{199}Hg/\Delta^{201}Hg$ ratios during specific Hg transformations in aerosols are needed to better understand fate of Hg and fractionation of Hg isotopes in aerosols.

3.4 PBM originated from atmospheric Hg(0) oxidation

Recent studies have explored the MIF variability of even-Hg isotopes (e.g., $\Delta^{200}Hg$), which is thought to be produced during photochemical Hg redox reactions at high altitudes and distinguishable among atmospheric Hg species (e.g., $\Delta^{200}Hg$ of Hg(0) *vs* GOM and wet deposition).[12, 20, 22, 75] $\Delta^{200}Hg$ has been used to track the pathways of atmospheric Hg deposition to Earth surface reservoirs.[21, 22, 76, 77] City-specific mean PBM $\Delta^{200}Hg$ obtained in the present study ranged from 0.02 to 0.06‰, while higher values (0.01 to 0.14‰) have been reported from rural areas in China (n = 3), a coastal site in the United States, and over oceans (Figure 5).[27-30] PBM in the atmosphere is sourced from primary anthropogenic PBM emissions, gas-particle partitioning of GOM emitted from anthropogenic sources, and gas-particle partitioning of GOM produced during atmospheric Hg(0) oxidation. PBM and GOM directly emitted from anthropogenic sources are expected to have $\Delta^{200}Hg$ values around 0.00 ± 0.03‰.[61, 78] The positive shift in the observed $\Delta^{200}Hg_{PBM}$ (the higher values than ~0.00‰ mentioned above) should be mainly caused by gas-particle partitioning of GOM produced by Hg(0) oxidation, which is observed to carry significantly positive $\Delta^{200}Hg$ values.[22, 27] Here we use $\Delta^{200}Hg$ to estimate the fraction of PBM sourced from atmospheric Hg(0) oxidation ($F_{Hg(0)\text{-}oxidation}$) based on Equations (3) and (4) below.

$$\Delta^{200}Hg_{sample} = F_{(anthropogenic)} \times \Delta^{200}H_{(PBM\&GOM\text{-}anthropogenic)} + F_{(Hg(0)\text{-}oxidation)} \times \Delta^{200}Hg_{(Hg(0)\text{-}oxidation)} \quad (3)$$

$$F_{(anthropogenic)} + F_{(Hg(0)\text{-}oxidation)} = 1 \quad (4)$$

where $\Delta^{200}Hg_{sample}$ is the observed $\Delta^{200}Hg$ values of PBM samples; $\Delta^{200}Hg_{(PBM\&GOM\text{-}anthropogenic)}$ is the $\Delta^{200}Hg$ values of anthropogenic emitted PBM and GOM; $\Delta^{200}Hg_{(Hg(0)\text{-}oxidation)}$ is the $\Delta^{200}Hg$ signature of GOM produced by Hg(0) oxidation; and $F_{(anthropogenic)}$ and $F_{(Hg(0)\text{-}oxidation)}$ are the fractions of PBM derived from anthropogenic emissions (PBM and gas-particle partitioning of GOM emitted from anthropogenic sources) and gaseous Hg(0) oxidation followed by gas-particle partitioning of GOM, respectively.

The $\Delta^{200}Hg$ signature of GOM produced by Hg(0) oxidation ($\Delta^{200}Hg_{(Hg(0)\text{-}oxidation)}$) is estimated to be 0.15 ± 0.06‰ based on observations in the free troposphere,[22] and this value is close to the

mean Δ^{200}Hg of precipitation at global background sites (0.16‰),[77] which is dominantly originated from removal of GOM produced in the free troposphere.[3, 79] Figure 5 shows the mean Δ^{200}Hg values of PBM, GOM, and precipitation at global sites excluding Polar region, where the near zero Δ^{200}Hg values of PBM are due to insufficient understanding of transformation mechanisms.[31, 32] Hence, the mean fractions (±1sd) of PBM sourced from atmospheric Hg(0) oxidation followed by gas-particle partitioning of GOM were estimated to be 41 ± 25%, 33 ± 22%, 53 ± 24%, 45 ± 26%, and 62 ± 24% in urban China, urban South Asia, rural China, Asian seas, and North American, respectively using Monte Carlo simulation (Text S2 and Figure S8). A combination of above results yields a mean fraction of 47% for the PBM sourced from atmospheric Hg(0) oxidation. This, together with the dominant contribution of Hg(0) oxidation to PBM in polar region,[32] suggests PBM is potentially an important sink for Hg(0) in the global atmosphere. For example, given the contributions of atmospheric Hg(0) oxidation to PBM and a total PBM deposition of 229 tons/yr in China,[36] we estimated that approximately 108 tons of Hg(0) in the atmosphere in China are removed annually via transformation to PBM, which accounts for 36% of the anthropogenic Hg(0) emissions in China.[51]

4 Environmental implications

Aerosols play a crucial role in the biogeochemical cycling of Hg in the atmosphere,[3, 8] but the knowledge concerning Hg chemistry in aerosols is limited.[7] PBM has been observed to frequently carry significantly positive Δ^{199}Hg values, which are clearly different from the corresponding signature for primary anthropogenic emissions.[23, 27, 28] Positive $\Delta^{199}Hg_{PBM}$ signatures together with a $\Delta^{199}Hg_{PBM}/\Delta^{201}Hg_{PBM}$ ratio of ~1.0 reported in previous studies indicate that photoreduction of Hg(II) occurred in aerosol,[24, 27, 28, 33] which is generally accounted for in modelling studies.[3, 8] In the present study, we found that the $\Delta^{199}Hg/\Delta^{201}Hg$ ratio varied largely from 0.94 to 1.39 in ten Chinese megacities and the ratio increased with the mean Δ^{199}Hg value in any individual city during the study period. We speculated that other reaction processes, including isotope exchange between Hg(II) and Hg(0), Hg(II) complexation with thiols, and photochemical oxidation of Hg(0) by reactive chloride in aerosols, are also potential factors influencing the odd-MIF of PBM in the present study. This is especially the case in urban atmosphere with elevated aerosol contents of chloride, Fe, and EC. This hypothesis could potentially explain the observed compounds of Hg in PBM[69] and the most abundant gaseous $HgCl_2$ compound simulated in the atmosphere.[8] Mercury chemistry in aerosols likely produces Hg compounds with different photochemical behaviors than those produced via gas-phase chemistry,[4, 8, 71] which therefore has a potential to influence the photochemistry of atmospheric Hg. It should be noted that the diagnostic $\Delta^{199}Hg/\Delta^{201}Hg$ ratios of PBM at many sites in this and previous studies resemble those of Hg(II) photoreduction,[23, 24, 27, 28]

indicating photoreduction of Hg(II) is likely the dominant mechanism inducing the positive PBM MIF in the continental atmosphere. It seems to be plausible that the Hg transformation processes in aerosols are largely influenced by aerosol chemistry and meteorological parameters, and the PBM isotope signatures imparted by these processes would differ noticeably in various atmospheric environments and over different time scales. The samples in the present study were collected during short sampling periods in several Chinese cities, and it is therefore not clear whether the proposed reaction processes in this study would be environmentally relevant for the aerosols in the global atmosphere. Further studies on PBM isotope signatures in various atmospheric environments (urban, remote, and oceanic) and over longer time scales are needed to improve our knowledge of the physiochemical reactions of Hg in aerosols.

There is an increasing consensus that Hg(0) in the atmosphere is more readily deposited to the Earth surface reservoir than traditionally assumed,[76, 77, 80, 81] however, missing atmospheric Hg oxidation processes may still exist in light of the fast photolysis of major constituents of gaseous oxidized Hg.[9] Based on the Δ^{200}Hg signatures of speciated atmospheric Hg, we estimate that an important fraction of PBM (~47% on global average) is sourced from Hg(0) oxidation followed by partitioning of GOM into aerosols. Deposition of PBM is an important pathway for the removal of atmospheric Hg,[34, 36] and therefore transformation of Hg(0) to PBM would constitute an important sink of atmospheric Hg(0). Previous studies have revealed that gas-particle partitioning of GOM, which is from both anthropogenic emission and Hg(0) oxidation, is an important source of PBM,[34] while the present study for the first time quantified the fraction of PBM sourced from the atmospheric Hg(0) oxidation process. We caution that, due to the insufficient knowledge of the isotope signatures of speciated atmospheric Hg, the quantification of the sources and transformation mechanisms of atmospheric Hg species have large uncertainties. Therefore, further intensive field and experimental studies on the fractionation of stable isotopes of speciated atmospheric Hg are still needed in order to better constrain the physicochemical processes of atmospheric Hg and the cycling of Hg between Earth surfaces and atmosphere.

■ Supporting Information

Additional information of the ancillary methodology, sampling locations, isotopic compositions of PBM, and relationship analysis between PBM isotopic compositions and ancillary parameters are presented in the Supporting Information (Text S1-S2, Table S1-S3, and Figure S1-S9).

■ Acknowledgements

This work was supported by the National Key R&D Program of China (2017YFC0212001),

the Key Research Program of Frontier Science, Chinese Academy of Sciences (ZDBS-LY-DQC029), the National Nature Science Foundation of China (41921004), and the K.C. Wong Education Foundation. We thank the following research groups for providing assistances in PBM sampling in their respective cities: Prof. Gan Zhang from Guangzhou Institute of Geochemistry, CAS, Guangzhou, China, Prof. Hai Guo from the Hong Kong Polytechnic University, Hong Kong, China, and Prof. Hong Gao from Lanzhou University, Lanzhou, China.

Figure 1 Means (±1sd) of δ^{202}Hg versus Δ^{199}Hg (A) and δ^{202}Hg versus Δ^{200}Hg (B) for PBM collected in the 10 megacities in this study. Observations of δ^{202}Hg, Δ^{199}Hg, and Δ^{200}Hg for PBM in rural areas of China,[28] oceans,[28-30], urban areas of South Asia,[25, 26] and USA,[27] as well as Hg(0) (GEM) in urban and rural areas of China[37, 52, 53] were also compiled from previous studies. Error bars are 1sd of the mean values.

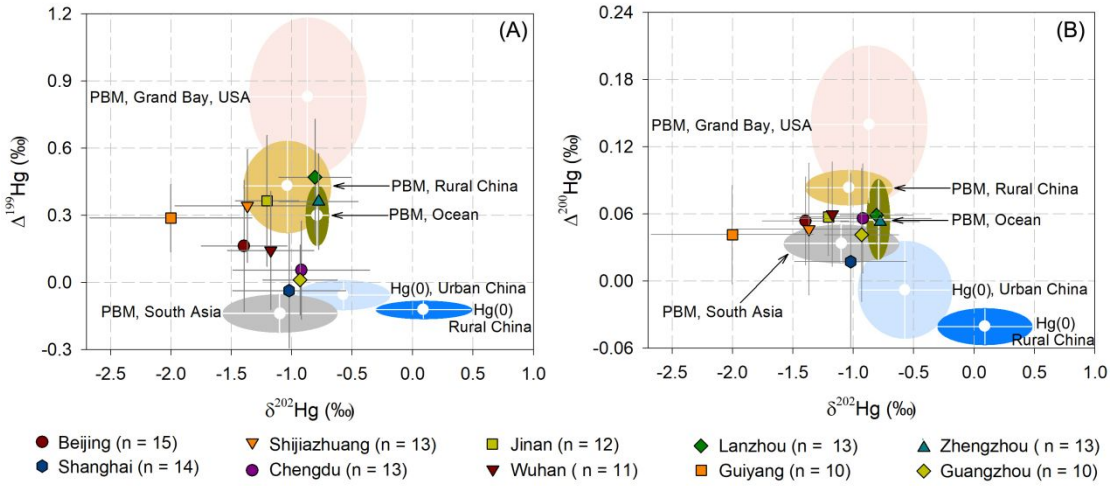

Figure 2 Summertime and wintertime means of PBM concentrations, PBM/$PM_{2.5}$ ratios, PBM/EC rations, $\delta^{202}Hg_{PBM}$, $\Delta^{199}Hg_{PBM}$, solar radiation, and air temperature at the 10 urban sites. Error bars are 1sd of the mean values.

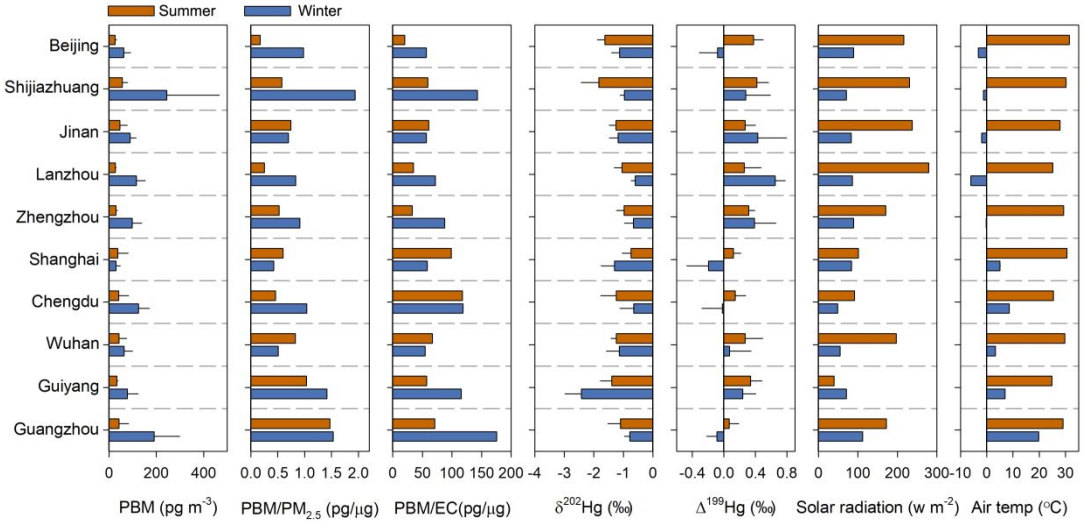

Figure 3 Linear regression analysis (Variables Entered - SPSS Statistics) between Δ^{199}Hg and Δ^{201}Hg of daily PBM samples in the 10 cities.

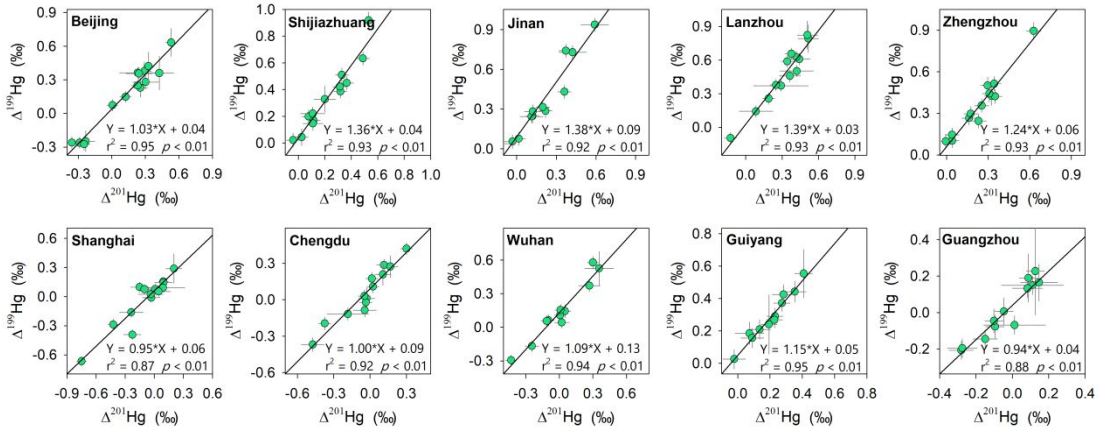

Figure 4 A diagram scheme showing the odd-MIF of PBM isotopes caused by potential physicochemical reactions in aerosols. GOM compounds produced from gaseous-phase Hg(0) oxidation are from previous studies.[4, 8] Photoreduction of Hg(II) in aerosols is expected to generate a $\Delta^{199}Hg/\Delta^{201}Hg$ ratio of ~1.0 and positive odd-MIF in reactant Hg(II) due to (+)MIE.[11, 56, 57, 62] We speculate that diagnostic $\Delta^{199}Hg/\Delta^{201}Hg$ ratios higher than 1.0 were caused by other heterogeneous Hg reactions in aerosols (e.g., complexation of Hg(II) with thiol (-SH), Hg(II)-Hg(0) isotope exchange, aqueous photooxidation of Hg(0) by reactive chloride) that express NVE.[12, 16, 18, 72]

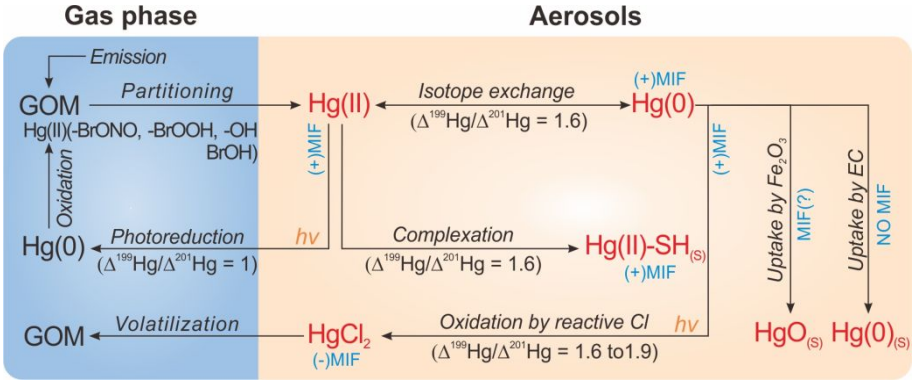

Figure 5 Summary of mean (±1sd) Δ^{200}Hg values of PBM, free tropospheric GOM, and background precipitation in different regions worldwide. Data are from this study and the literature.[22, 25-30, 77] Green circles indicate the mean PBM Δ^{200}Hg values at individual sites (n = 20).

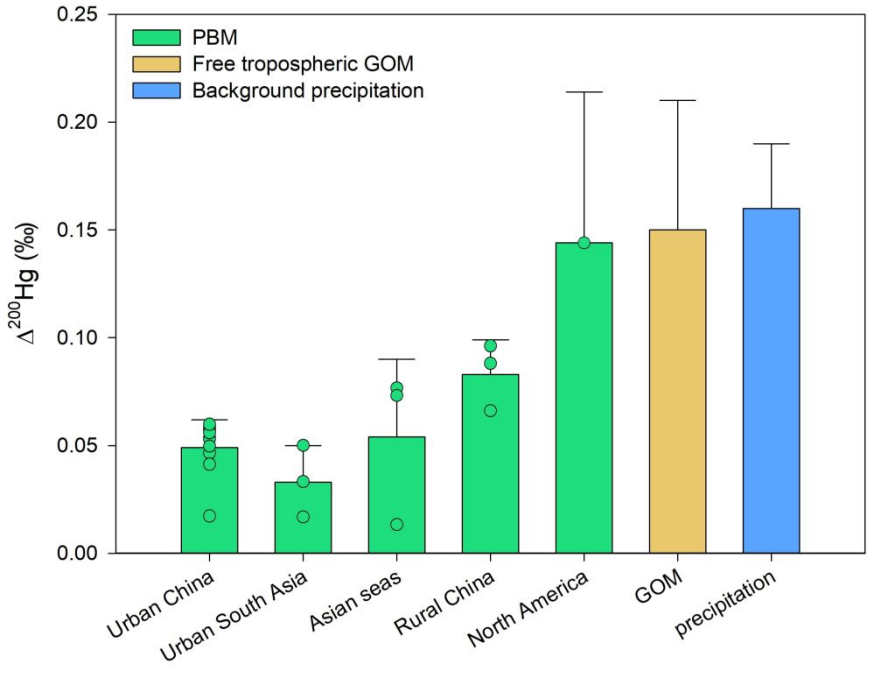

References:

1. Gustin, M.; Jaffe, D., Reducing the Uncertainty in Measurement and Understanding of Mercury in the Atmosphere. *Environmental Science & Technology* **2010,** *44*, (7), 2222-2227.

2. Holmes, C. D.; Jacob, D. J.; Corbitt, E. S.; Mao, J.; Yang, X.; Talbot, R.; Slemr, F., Global atmospheric model for mercury including oxidation by bromine atoms. *Atmos Chem Phys* **2010,** *10*, (24), 12037-12057.

3. Horowitz, H. M.; Jacob, D. J.; Zhang, Y. X.; Dibble, T. S.; Slemr, F.; Amos, H. M.; Schmidt, J. A.; Corbitt, E. S.; Marais, E. A.; Sunderland, E. M., A new mechanism for atmospheric mercury redox chemistry: implications for the global mercury budget. *Atmos Chem Phys* **2017,** *17*, (10), 6353-6371.

4. Saiz-Lopez, A.; Sitkiewicz, S. P.; Roca-Sanjuan, D.; Oliva-Enrich, J. M.; Davalos, J. Z.; Notario, R.; Jiskra, M.; Xu, Y.; Wang, F.; Thackray, C. P.; Sunderland, E. M.; Jacob, D. J.; Travnikov, O.; Cuevas, C. A.; Acuna, A. U.; Rivero, D.; Plane, J. M. C.; Kinnison, D. E.; Sonke, J. E., Photoreduction of gaseous oxidized mercury changes global atmospheric mercury speciation, transport and deposition. *Nat Commun* **2018,** *9*, (1), 4796.

5. Obrist, D.; Tas, E.; Peleg, M.; Matveev, V.; Fain, X.; Asaf, D.; Luria, M., Bromine-induced oxidation of mercury in the mid-latitude atmosphere. *Nat Geosci* **2011,** *4*, (1), 22-26.

6. Lyman, S. N.; Jaffe, D. A., Formation and fate of oxidized mercury in the upper troposphere and lower stratosphere. *Nat Geosci* **2012,** *5*, (2), 114-117.

7. Ariya, P. A.; Amyot, M.; Dastoor, A.; Deeds, D.; Feinberg, A.; Kos, G.; Poulain, A.; Ryjkov, A.; Semeniuk, K.; Subir, M.; Toyota, K., Mercury Physicochemical and Biogeochemical Transformation in the Atmosphere and at Atmospheric Interfaces: A Review and Future

476 Directions. *Chem Rev* **2015,** *115*, (10), 3760-3802.

477 8. Shah, V.; Jacob, D. J.; Thackray, C. P.; Wang, X.; Sunderland, E. M.; Dibble, T. S.; Saiz-
478 Lopez, A.; Cernusak, I.; Kello, V.; Castro, P. J.; Wu, R.; Wang, C., Improved Mechanistic Model
479 of the Atmospheric Redox Chemistry of Mercury. *Environ Sci Technol* **2021,** *55*, (21), 14445-
480 14456.

481 9. Saiz-Lopez, A.; Travnikov, O.; Sonke, J. E.; Thackray, C. P.; Jacob, D. J.; Carmona-Garcia,
482 J.; Frances-Monerris, A.; Roca-Sanjuan, D.; Acuna, A. U.; Davalos, J. Z.; Cuevas, C. A.; Jiskra,
483 M.; Wang, F. Y.; Bieser, J.; Plane, J. M. C.; Francisco, J. S., Photochemistry of oxidized Hg(I)
484 and Hg(II) species suggests missing mercury oxidation in the troposphere. *P Natl Acad Sci*
485 *USA* **2020,** *117*, (49), 30949-30956.

486 10. Blum, J. D.; Sherman, L. S.; Johnson, M. W., Mercury isotopes in earth and environmental
487 sciences. *Annu Rev Earth Pl Sc* **2014,** *42*, 249-269.

488 11. Bergquist, B. A.; Blum, J. D., Mass-dependent and -independent fractionation of Hg
489 isotopes by photoreduction in aquatic systems. *Science* **2007,** *318*, (5849), 417-420.

490 12. Sun, G.; Sommar, J.; Feng, X.; Lin, C.-J.; Ge, M.; Wang, W.; Yin, R.; Fu, X.; Shang, L.,
491 Mass-dependent and -independent fractionation of mercury isotope during gas-phase oxidation
492 of elemental mercury vapor by atomic Cl and Br. *Environmental Science & Technology* **2016,**
493 *50*, (17), 9232-9241.

494 13. Zheng, W.; Hintelmann, H., Mercury isotope fractionation during photoreduction in natural
495 water is controlled by its Hg/DOC ratio. *Geochim Cosmochim Ac* **2009,** *73*, (22), 6704-6715.

496 14. Motta, L. C.; Blum, J. D.; Johnson, M. W.; Umhau, B. P.; Popp, B. N.; Washburn, S. J.;
497 Drazen, J. C.; Benitez-Nelson, C. R.; Hannides, C. C. S.; Close, H. G.; Lamborg, C. H., Mercury

498 Cycling in the North Pacific Subtropical Gyre as Revealed by Mercury Stable Isotope Ratios.
499 *Global Biogeochem Cy* **2019,** *33*, (6), 777-794.
500 15. Sherman, L. S.; Blum, J. D.; Johnson, K. P.; Keeler, G. J.; Barres, J. A.; Douglas, T. A.,
501 Mass-independent fractionation of mercury isotopes in Arctic snow driven by sunlight. *Nat*
502 *Geosci* **2010,** *3*, (3), 173-177.
503 16. Wiederhold, J. G.; Cramer, C. J.; Daniel, K.; Infante, I.; Bourdon, B.; Kretzschmar, R.,
504 Equilibrium Mercury Isotope Fractionation between Dissolved Hg(II) Species and Thiol-Bound
505 Hg. *Environmental Science & Technology* **2010,** *44*, (11), 4191-4197.
506 17. Zheng, W.; Hintelmann, H., Nuclear Field Shift Effect in Isotope Fractionation of Mercury
507 during Abiotic Reduction in the Absence of Light. *J Phys Chem A* **2010,** *114*, (12), 4238-4245.
508 18. Zheng, W.; Demers, J. D.; Lu, X.; Bergquist, B. A.; Anbar, A. D.; Blum, J. D.; Gu, B.,
509 Mercury Stable Isotope Fractionation during Abiotic Dark Oxidation in the Presence of Thiols
510 and Natural Organic Matter. *Environ Sci Technol* **2019,** *53*, (4), 1853-1862.
511 19. Gratz, L. E.; Keeler, G. J.; Blum, J. D.; Sherman, L. S., Isotopic composition and
512 fractionation of mercury in Great Lakes precipitation and ambient air. *Environmental Science &*
513 *Technology* **2010,** *44*, (20), 7764-7770.
514 20. Chen, J. B.; Hintelmann, H.; Feng, X. B.; Dimock, B., Unusual fractionation of both odd
515 and even mercury isotopes in precipitation from Peterborough, ON, Canada. *Geochim*
516 *Cosmochim Ac* **2012,** *90*, 33-46.
517 21. Demers, J. D.; Blum, J. D.; Zak, D. R., Mercury isotopes in a forested ecosystem:
518 Implications for air-surface exchange dynamics and the global mercury cycle. *Global*
519 *Biogeochem Cy* **2013,** *27*, (1), 222-238.

22. Fu, X.; Jiskra, M.; Yang, X.; Marusczak, N.; Enrico, M.; Chmeleff, J.; Heimbürger-Boavida, L.-E.; Gheusi, F.; Sonke, J. E., Mass-Independent Fractionation of Even and Odd Mercury Isotopes during Atmospheric Mercury Redox Reactions. *Environmental Science & Technology* **2021,** *55*, (14), 10164-10174.

23. Huang, Q.; Chen, J. B.; Huang, W. L.; Fu, P. Q.; Guinot, B.; Feng, X. B.; Shang, L. H.; Wang, Z. H.; Wang, Z. W.; Yuan, S. L.; Cai, H. M.; Wei, L. F.; Yu, B., Isotopic composition for source identification of mercury in atmospheric fine particles. *Atmos Chem Phys* **2016,** *16*, (18), 11773-11786.

24. Xu, H. M.; Sun, R. Y.; Cao, J. J.; Huang, R.-J.; Guinot, B.; Shen, Z. X.; Jiskra, M.; Li, C. X.; Du, B. Y.; He, C.; Liu, S. X.; Zhang, T.; Sonke, J. E., Mercury stable isotope compositions of Chinese urban fine particulates in winter haze days: Implications for Hg sources and transformations. *Chem Geol* **2019,** *504*, 267-275.

25. Das, R.; Wang, X. F.; Khezri, B.; Webster, R. D.; Sikdar, P. K.; Datta, S., Mercury isotopes of atmospheric particle bound mercury for source apportionment study in urban Kolkata, India. *Elementa-Sci Anthrop* **2016,** *4*, 1-12.

26. Guo, J.; Sharma, C. M.; Tripathee, L.; Kang, S.; Fu, X.; Huang, J.; Shrestha, K. L.; Chen, P., Source identification of atmospheric particle-bound mercury in the Himalayan foothills through non-isotopic and isotope analyses. *Environ Pollut* **2021,** *286*, 117317.

27. Rolison, J. M.; Landing, W. M.; Luke, W.; Cohen, M.; Salters, V. J. M., Isotopic composition of species-specific atmospheric Hg in a coastal environment. *Chem Geol* **2013,** *336*, 37-49.

28. Fu, X. W.; Zhang, H.; Feng, X. B.; Tan, Q. Y.; Ming, L. L.; Liu, C.; Zhang, L. M., Domestic and Transboundary Sources of Atmospheric Particulate Bound Mercury in Remote Areas of

China: Evidence from Mercury Isotopes. *Environmental Science & Technology* **2019,** *53*, (4), 1947-1957.

29. Yu, B.; Yang, L.; Wang, L. L.; Liu, H. W.; Xiao, C. L.; Liang, Y.; Liu, Q.; Yin, Y. G.; Hu, L. G.; Shi, J. B.; Jiang, G. B., New evidence for atmospheric mercury transformations in the marine boundary layer from stable mercury isotopes. *Atmos Chem Phys* **2020,** *20*, (16), 9713-9723.

30. Qiu, Y.; Gai, P.; Yue, F.; Zhang, Y.; He, P.; Kang, H.; Yu, X.; Lam, P. K. S.; Chen, J.; Xie, Z., Stable Mercury Isotopes Revealing Photochemical Processes in the Marine Boundary Layer. *Journal of Geophysical Research: Atmospheres* **2021,** *126*, (16), e2021JD034630.

31. Li, C.; Chen, J.; Angot, H.; Zheng, W.; Shi, G.; Ding, M.; Du, Z.; Zhang, Q.; Ma, X.; Kang, S.; Xiao, C.; Ren, J.; Qin, D., Seasonal Variation of Mercury and Its Isotopes in Atmospheric Particles at the Coastal Zhongshan Station, Eastern Antarctica. *Environmental Science & Technology* **2020,** *54*, (18), 11344-11355.

32. Zheng, W.; Chandan, P.; Steffen, A.; Stupple, G.; De Vera, J.; Mitchell, C. P. J.; Wania, F.; Bergquist, B. A., Mercury stable isotopes reveal the sources and transformations of atmospheric Hg in the high Arctic. *Appl Geochem* **2021,** *131*, 105002.

33. Huang, Q.; Chen, J. B.; Huang, W. L.; Reinfelder, J. R.; Fu, P. Q.; Yuan, S. L.; Wang, Z. W.; Yuan, W.; Cai, H. M.; Ren, H.; Sun, Y. L.; He, L., Diel variation in mercury stable isotope ratios records photoreduction of PM2.5-bound mercury. *Atmos Chem Phys* **2019,** *19*, (1), 315-325.

34. Amos, H. M.; Jacob, D. J.; Holmes, C. D.; Fisher, J. A.; Wang, Q.; Yantosca, R. M.; Corbitt, E. S.; Galarneau, E.; Rutter, A. P.; Gustin, M. S.; Steffen, A.; Schauer, J. J.; Graydon, J. A.; St Louis, V. L.; Talbot, R. W.; Edgerton, E. S.; Zhang, Y.; Sunderland, E. M., Gas-particle

partitioning of atmospheric Hg(II) and its effect on global mercury deposition. *Atmos Chem Phys* **2012,** *12*, (1), 591-603.

35. Fu, X. W.; Zhang, H.; Yu, B.; Wang, X.; Lin, C. J.; Feng, X. B., Observations of atmospheric mercury in China: a critical review. *Atmos Chem Phys* **2015,** *15*, (16), 9455-9476.

36. Wang, X.; Lin, C. J.; Feng, X. B.; Yuan, W.; Fu, X. W.; Zhang, H.; Wu, Q. R.; Wang, S. X., Assessment of Regional Mercury Deposition and Emission Outflow in Mainland China. *J Geophys Res-Atmos* **2018,** *123*, (17), 9868-9890.

37. Fu, X.; Liu, C.; Zhang, H.; Xu, Y.; Zhang, H.; Li, J.; Lyu, X.; Zhang, G.; Guo, H.; Wang, X.; Zhang, L.; Feng, X., Isotopic compositions of atmospheric total gaseous mercury in 10 Chinese cities and implications for land surface emissions. *Atmos. Chem. Phys.* **2021,** *21*, (9), 6721-6734.

38. Fu, X. W.; Heimburger, L. E.; Sonke, J. E., Collection of atmospheric gaseous mercury for stable isotope analysis using iodine- and chlorine-impregnated activated carbon traps. *J Anal Atom Spectrom* **2014,** *29*, (5), 841-852.

39. Blum, J. D.; Bergquist, B. A., Reporting of variations in the natural isotopic composition of mercury. *Anal Bioanal Chem* **2007,** *388*, (2), 353-359.

40. Blum, J. D.; Johnson, M. W., Recent Developments in Mercury Stable Isotope Analysis. *Reviews in Mineralogy & Geochemistry* **2017,** *82*, 733-757.

41. Ming, L. L.; Jin, L.; Li, J.; Fu, P. Q.; Yang, W. Y.; Liu, D.; Zhang, G.; Wang, Z. F.; Li, X. D., PM2.5 in the Yangtze River Delta, China: Chemical compositions, seasonal variations, and regional pollution events. *Environ Pollut* **2017,** *223*, 200-212.

42. Mao, H. T.; Cheng, I.; Zhang, L. M., Current understanding of the driving mechanisms for

586 spatiotemporal variations of atmospheric speciated mercury: a review. *Atmos Chem Phys* **2016,**
587 *16*, (20), 12897-12924.
588 43. Åkerblom, S.; Meili, M.; Bishop, K., Organic Matter in Rain: An Overlooked Influence on
589 Mercury Deposition. *Environmental Science & Technology Letters* **2015,** *2*, (4), 128-132.
590 44. Benoit, J. M.; Mason, R. P.; Gilmour, C. C.; Aiken, G. R., Constants for mercury binding
591 by dissolved organic matter isolates from the Florida Everglades. *Geochimica et Cosmochimica*
592 *Acta* **2001,** *65*, (24), 4445-4451.
593 45. Rutter, A. P.; Schauer, J. J., The impact of aerosol composition on the particle to gas
594 partitioning of reactive mercury. *Environmental Science & Technology* **2007,** *41*, (11), 3934-
595 3939.
596 46. Xu, H.; Sonke, J. E.; Guinot, B.; Fu, X.; Sun, R.; Lanzanova, A.; Candaudap, F.; Shen, Z.;
597 Cao, J., Seasonal and Annual Variations in Atmospheric Hg and Pb Isotopes in Xi'an, China.
598 *Environ Sci Technol* **2017,** *51*, (7), 3759-3766.
599 47. Yu, B.; Fu, X.; Yin, R.; Zhang, H.; Wang, X.; Lin, C.-J.; Wu, C.; Zhang, Y.; He, N.; Fu, P.;
600 Wang, Z.; Shang, L.; Sommar, J.; Sonke, J. E.; Maurice, L.; Guinot, B.; Feng, X., Isotopic
601 Composition of Atmospheric Mercury in China: New Evidence for Sources and Transformation
602 Processes in Air and in Vegetation. *Environmental Science & Technology* **2016,** *50*, (17), 9262-
603 9269.
604 48. Tang, S.; Feng, C.; Feng, X.; Zhu, J.; Sun, R.; Fan, H.; Wang, L.; Li, R.; Mao, T.; Zhou, T.,
605 Stable isotope composition of mercury forms in flue gases from a typical coal-fired power plant,
606 Inner Mongolia, northern China. *J Hazard Mater* **2017,** *328*, 90-97.
607 49. Li, X. Y.; Li, Z. G.; Chen, J.; Zhang, L. M.; Yin, R. S.; Sun, G. Y.; Meng, B.; Cui, Z. K.; Feng,

608 X. B., Isotope signatures of atmospheric mercury emitted from residential coal combustion.
609 *Atmos Environ* **2021,** *246*, 118175.
610 50. Li, X.; Chen, J.; Tang, L.; Wu, T.; Fu, C.; Li, Z.; Sun, G.; Zhao, H.; Zhang, L.; Li, Q.; Feng,
611 X., Mercury isotope signatures of a pre-calciner cement plant in Southwest China. *J Hazard*
612 *Mater* **2021,** *401*, 123384.
613 51. Zhang, L.; Wang, S. X.; Wang, L.; Wu, Y.; Duan, L.; Wu, Q. R.; Wang, F. Y.; Yang, M.;
614 Yang, H.; Hao, J. M.; Liu, X., Updated Emission Inventories for Speciated Atmospheric Mercury
615 from Anthropogenic Sources in China. *Environmental Science & Technology* **2015,** *49*, (5),
616 3185-3194.
617 52. Fu, X.; Yang, X.; Tan, Q.; Ming, L.; Lin, T.; Lin, C.-J.; Li, X.; Feng, X., Isotopic Composition
618 of Gaseous Elemental Mercury in the Marine Boundary Layer of East China Sea. *Journal of*
619 *Geophysical Research: Atmospheres* **2018,** *123*, (14), 7656-7669.
620 53. Fu, X.; Zhang, H.; Liu, C.; Zhang, H.; Lin, C.-J.; Feng, X., Significant Seasonal Variations
621 in Isotopic Composition of Atmospheric Total Gaseous Mercury at Forest Sites in China Caused
622 by Vegetation and Mercury Sources. *Environmental Science & Technology* **2019,** *53*, (23),
623 13748-13756.
624 54. Turpin, B. J.; Huntzicker, J. J., Identification of Secondary Organic Aerosol Episodes and
625 Quantitation of Primary and Secondary Organic Aerosol Concentrations during Scaqs. *Atmos*
626 *Environ* **1995,** *29*, (23), 3527-3544.
627 55. Tian, H. Z.; Zhu, C. Y.; Gao, J. J.; Cheng, K.; Hao, J. M.; Wang, K.; Hua, S. B.; Wang, Y.;
628 Zhou, J. R., Quantitative assessment of atmospheric emissions of toxic heavy metals from
629 anthropogenic sources in China: historical trend, spatial distribution, uncertainties, and control

policies. *Atmos. Chem. Phys.* **2015,** *15*, (17), 10127-10147.

56. Zheng, W.; Hintelmann, H., Isotope fractionation of mercury during its photochemical reduction by low-molecular-weight organic compounds. *J Phys Chem A* **2010,** *114*, (12), 4246-53.

57. Huang, Q.; He, X.; Huang, W.; Reinfelder, J. R., Mass-Independent Fractionation of Mercury Isotopes during Photoreduction of Soot Particle Bound Hg(II). *Environmental Science & Technology* **2021**.

58. Seigneur, C.; Wrobel, J.; Constantinou, E., A Chemical Kinetic Mechanism for Atmospheric Inorganic Mercury. *Environmental Science & Technology* **1994,** *28*, (9), 1589-1597.

59. Seigneur, C.; Abeck, H.; Chia, G.; Reinhard, M.; Bloom, N. S.; Prestbo, E.; Saxena, P., Mercury adsorption to elemental carbon (soot) particles and atmospheric particulate matter. *Atmos Environ* **1998,** *32*, (14-15), 2649-2657.

60. Rutter, A. P.; Shakya, K. M.; Lehr, R.; Schauer, J. J.; Griffin, R. J., Oxidation of gaseous elemental mercury in the presence of secondary organic aerosols. *Atmos Environ* **2012,** *59*, 86-92.

61. Sun, R. Y.; Streets, D. G.; Horowitz, H. M.; Amos, H. M.; Liu, G. J.; Perrot, V.; Toutain, J. P.; Hintelmann, H.; Sunderland, E. M.; Sonke, J. E., Historical (1850–2010) mercury stable isotope inventory from anthropogenic sources to the atmosphere. *Elem. Sci. Anth* **2016,** *4*, (91), 1-15.

62. Motta, L. C.; Kritee, K.; Blum, J. D.; Tsz-Ki Tsui, M.; Reinfelder, J. R., Mercury Isotope Fractionation during the Photochemical Reduction of Hg(II) Coordinated with Organic Ligands. *The Journal of Physical Chemistry A* **2020,** *124*, (14), 2842-2853.

652 63. Zhang, H.; Tan, Q.; Zhang, L.; Fu, X.; Feng, X., A Laboratory Study on the Isotopic
653 Composition of Hg(0) Emitted From Hg-Enriched Soils in Wanshan Hg Mining Area. *Journal of*
654 *Geophysical Research: Atmospheres* **2020,** *125*, (19), e2020JD032572.
655 64. Pio, C. A.; Legrand, M.; Oliveira, T.; Afonso, J.; Santos, C.; Caseiro, A.; Fialho, P.; Barata,
656 F.; Puxbaum, H.; Sanchez-Ochoa, A.; Kasper-Giebl, A.; Gelencser, A.; Preunkert, S.; Schock,
657 M., Climatology of aerosol composition (organic versus inorganic) at nonurban sites on a west-
658 east transect across Europe. *J Geophys Res-Atmos* **2007,** *112*, D23S02.
659 65. Tong, Y.; Eichhorst, T.; Olson, M. R.; McGinnis, J. E.; Turner, I.; Rutter, A. P.; Shafer, M.
660 M.; Wang, X.; Schauer, J. J., Atmospheric photolytic reduction of Hg(ii) in dry aerosols.
661 *Environmental Science: Processes & Impacts* **2013,** *15*, (10), 1883-1888.
662 66. Lin, C. J.; Pehkonen, S. O., Aqueous free radical chemistry of mercury in the presence of
663 iron oxides and ambient aerosol. *Atmos Environ* **1997,** *31*, (24), 4125-4137.
664 67. Li, W. J.; Shao, L. Y.; Zhang, D. Z.; Ro, C. U.; Hu, M.; Bi, X. H.; Geng, H.; Matsuki, A.; Niu,
665 H. Y.; Chen, J. M., A review of single aerosol particle studies in the atmosphere of East Asia:
666 morphology, mixing state, source, and heterogeneous reactions. *J Clean Prod* **2016,** *112*, 1330-
667 1349.
668 68. Mason, R. P.; Lawson, N. M.; Sheu, G. R., Mercury in the Atlantic Ocean: factors
669 controlling air-sea exchange of mercury and its distribution in the upper waters. *Deep-Sea Res*
670 *Pt Ii* **2001,** *48*, (13), 2829-2853.
671 69. Feng, X. B.; Lu, J. Y.; Gregoire, D. C.; Hao, Y. J.; Banic, C. M.; Schroeder, W. H., Analysis
672 of inorganic mercury species associated with airborne particulate matter/aerosols: method
673 development. *Anal Bioanal Chem* **2004,** *380*, (4), 683-689.

674 70. Wang, Y.; Liu, G.; Li, Y.; Liu, Y.; Guo, Y.; Shi, J.; Hu, L.; Cai, Y.; Yin, Y.; Jiang, G.,
675 Occurrence of Mercurous [Hg(I)] Species in Environmental Solid Matrices as Probed by Mild 2-
676 Mercaptoethanol Extraction and HPLC-ICP-MS Analysis. *Environmental Science & Technology*
677 *Letters* **2020,** *7*, (7), 482-488.
678 71. Jiang, T.; Skyllberg, U.; Wei, S. Q.; Wang, D. Y.; Lu, S.; Jiang, Z. M.; Flanagan, D. C.,
679 Modeling of the structure-specific kinetics of abiotic, dark reduction of Hg(II) complexed by O/N
680 and S functional groups in humic acids while accounting for time-dependent structural
681 rearrangement. *Geochim Cosmochim Ac* **2015,** *154*, 151-167.
682 72. Stathopoulos, D. Fractionation of mercury isotopes in an aqueous environment: Chemical
683 Oxidation. Master Thesis, Trent University, Peterborough, Ontario, Canada, 2014.
684 73. Fu, B.; Sun, R.; Yao, H.; Hower, J. C.; Yuan, J.; Luo, G.; Hu, H.; Mardon, S. M.; Tang, Q.,
685 Mercury stable isotope fractionation during gaseous elemental mercury adsorption onto coal fly
686 ash particles: Experimental and field observations. *J Hazard Mater* **2021,** *405*, 124280.
687 74. Kurien, U.; Hu, Z. Z.; Lee, H.; Dastoor, A. P.; Ariya, P. A., Radiation enhanced uptake of
688 Hg-(g)(o) on iron (oxyhydr) oxide nanoparticles. *Rsc Advances* **2017,** *7*, (71), 45010-45021.
689 75. Kwon, S. Y.; Blum, J. D.; Yin, R.; Tsui, M. T. K.; Yang, Y. H.; Choi, J. W., Mercury stable
690 isotopes for monitoring the effectiveness of the Minamata Convention on Mercury. *Earth-*
691 *Science Reviews* **2020,** *203*, 103111.
692 76. Enrico, M.; Le Roux, G.; Marusczak, N.; Heimburger, L. E.; Claustres, A.; Fu, X. W.; Sun,
693 R. Y.; Sonke, J. E., Atmospheric Mercury Transfer to Peat Bogs Dominated by Gaseous
694 Elemental Mercury Dry Deposition. *Environmental Science & Technology* **2016,** *50*, (5), 2405-
695 2412.

77. Jiskra, M.; Heimbürger-Boavida, L.-E.; Desgranges, M.-M.; Petrova, M. V.; Dufour, A.; Ferreira-Araujo, B.; Masbou, J.; Chmeleff, J.; Thyssen, M.; Point, D.; Sonke, J. E., Mercury stable isotopes constrain atmospheric sources to the ocean. *Nature* **2021,** *597*, (7878), 678-682.

78. Sun, R. Y.; Jiskra, M.; Amos, H. M.; Zhang, Y. X.; Sunderland, E. M.; Sonke, J. E., Modelling the mercury stable isotope distribution of Earth surface reservoirs: Implications for global Hg cycling. *Geochim Cosmochim Ac* **2019,** *246*, 156-173.

79. Selin, N. E.; Jacob, D. J., Seasonal and spatial patterns of mercury wet deposition in the United States: Constraints on the contribution from North American anthropogenic sources. *Atmos Environ* **2008,** *42*, (21), 5193-5204.

80. Obrist, D.; Agnan, Y.; Jiskra, M.; Olson, C. L.; Colegrove, D. P.; Hueber, J.; Moore, C. W.; Sonke, J. E.; Helmig, D., Tundra uptake of atmospheric elemental mercury drives Arctic mercury pollution. *Nature* **2017,** *547*, (7662), 201-204.

81. Zheng, W.; Obrist, D.; Weis, D.; Bergquist, B. A., Mercury isotope compositions across North American forests. *Global Biogeochem Cy* **2016,** *30*, (10), 1475-1492.